Journal of Solid State Chemistry 238 (2016) 121–128

Contents lists available at ScienceDirect

Journal of Solid State Chemistry

journal homepage: www.elsevier.com/locate/jssc

New series of triple molybdates $AgA_3R(MoO_4)_5$ (A=Mg, R=Cr, Fe; A=Mn, R=Al, Cr, Fe, Sc, In) with framework structures and mobile silver ion sublattices

Irina Yu. Kotova [a,b], Sergey F. Solodovnikov [c,d], Zoya A. Solodovnikova [c], Dmitry A. Belov [e], Sergey Yu. Stefanovich [e], Aleksandra A. Savina [a,b,*], Elena G. Khaikina [a,b]

[a] Baikal Institute of Nature Management, Siberian Branch, Russian Academy of Sciences, Sakh'yanova St. 6, Ulan-Ude 670047, Buryat Republic, Russia
[b] Buryat State University, Smolin St. 24a, Ulan-Ude 670000, Buryat Republic, Russia
[c] Nikolaev Institute of Inorganic Chemistry, Siberian Branch, Russian Academy of Sciences, Acad. Lavrentiev Ave. 3, Novosibirsk 630090, Russia
[d] Novosibirsk State University, Pirogov St. 2, Novosibirsk 630090, Russia
[e] Lomonosov Moscow State University, Leninskie Gory 1, Moscow 119991, Russia

ARTICLE INFO

Article history:
Received 10 December 2015
Received in revised form
28 February 2016
Accepted 1 March 2016
Available online 4 March 2016

Keywords:
Triple molybdates
Silver
Synthesis
Structure
Ionic conductivity.

ABSTRACT

Triple molybdates $AgA_3R(MoO_4)_5$ (A=Mg, R=Cr, Fe; A=Mn, R=Al, Cr, Fe, Sc, In) of the $NaMg_3In(MoO_4)_5$ type were synthesized and single crystals of $AgMg_3R(MoO_4)_5$ (R=Cr, Fe) were grown. In their structures, the MoO_4 tetrahedra, pairs and trimers of edge-shared (Mg, R)O_6 octahedra are connected by common vertices to form a 3D framework. Large framework cavities involve Ag^+ cations disordered on three nearby positions with CN=3+1 or 4+1. Alternating (Mg, R)O_6 octahedra and MoO_4 tetrahedra in the framework form quadrangular windows penetrable for Ag^+ at elevated temperatures. Above 653–673 K, the newly obtained molybdates demonstrate abrupt reduction of the activation energy to 0.4–0.6 eV. At 773 K, $AgMg_3Al(MoO_4)_5$ shows electric conductivity $2.5 \cdot 10^{-2}$ S/cm and E_a=0.39 eV compatible with characteristics of the best ionic conductors of the NASICON type.

1. Introduction

In the systems containing molybdates of sodium, di- and trivalent metals, there are two groups of triple molybdates, $Na_{1-x}A_{1-x}R_{1+x}(MoO_4)_3$ and $NaA_3R(MoO_4)_5$, crystallizing in the structure types of NASICON [1] and $NaMg_3In(MoO_4)_5$ [2–6], respectively. Both structures do exist in the ternary molybdate systems involving cations of trivalent metals with $r(R^{3+}) < 1$ Å.

In view of close ionic radii of Na^+ and Ag^+, the formation of analogous phases in similar silver containing systems is rather probable. Indeed, studying the systems Ag_2MoO_4–$AMoO_4$–$R_2(MoO_4)_3$ (A=Mg, Co, R=Al; A=Mg, R=In), we have observed the formation of rhombohedral phases $Ag_{1-x}A_{1-x}R_{1+x}(MoO_4)_3$ of the NASICON type with wide homogeneity ranges, as well as triclinic triple molybdates $AgA_3R(MoO_4)_5$ of the $NaMg_3In(MoO_4)_5$ type [7–9]. The phase formation features of those triple molybdates may be illustrated with an example of Ag_2MoO_4–$MgMoO_4$–$Al_2(MoO_4)_3$ system studied by us at 773 K [8]. Because of a partial nonquasibinarity of the boundary system Ag_2MoO_4–$Al_2(MoO_4)_3$, the limited area $Ag_2Mg_2(MoO_4)_3$–$MgMoO_4$–$Al_2(MoO_4)_3$–$AgAl(MoO_4)_2$ was investigated (Fig. 1) where formation of triple molybdates $AgMgAl(MoO_4)_3$ of the NASICON type and $AgMg_3Al(MoO_4)_5$ (S_2) of the $NaMg_3In(MoO_4)_5$ type has been established. As seen in Fig. 1, the S_2 compound has no noticeable homogeneity range along the $AgAl(MoO_4)_2$–$MgMoO_4$ join. On the contrary, the phase of variable composition $Ag_{1-x}Mg_{1-x}Al_{1+x}(MoO_4)_3$ with x up to 0.4 (S_1) is formed as a solid solution extending along the join $AgMgAl(MoO_4)_3$–$Al_2(MoO_4)_3$.

Silver-containing $Ag_{1-x}A_{1-x}R_{1+x}(MoO_4)_3$ phases [10] with rhombohedral NASICON-like structures demonstrated high ionic conductivity typical for many representatives of this structural family. In the family of $NaMg_3In(MoO_4)_5$, the structure – property correlations were not earlier examined, and the present paper is the first step in this direction. Thus, the subject of the paper is preparation, structure determination and characterization of electro-conductive properties of triclinic triple molybdates $AgA_3R(MoO_4)_5$ (A=Mg, R=Cr, Fe; A=Mn, R=Al, Cr, Fe, Sc, In) crystallizing in the $NaMg_3In(MoO_4)_5$ structure.

2. Experimental section

Starting simple molybdates were obtained by gradual annealing of stoichiometric mixtures of $AgNO_3$ (analytical grade), MgO

* Corresponding author at: Baikal Institute of Nature Management, Siberian Branch, Russian Academy of Sciences, Sakh'yanova St. 6, Ulan-Ude 670047, Buryat Republic, Russia
E-mail address: alex551112@mail.ru (A.A. Savina).

http://dx.doi.org/10.1016/j.jssc.2016.03.003
0022-4596/

(reagent grade), MnO (chemically pure), $R(NO_3)_3 \cdot 9H_2O$, R=Al, Fe, Cr (analytical grade), Sc_2O_3 (reagent grade), In_2O_3 (reagent grade), and MoO_3 (reagent grade) at 623–723 K for Ag_2MoO_4, 673–1023 K for $MgMoO_4$, 623–973 K for $MnMoO_4$, 573–973(1023) K for $R_2(MoO_4)_3$ (R=Al, Fe, Cr), and 673–1073 K for $R_2(MoO_4)_3$ (R=Sc, In), respectively. As a flux for growing single crystals of triple molybdates, we used $Ag_2Mo_2O_7$ synthesized by annealing of the mixture $Ag_2MoO_4+2MoO_3$ at 573–663 K. Powder XRD and thermal characteristics of all prepared compounds agree well with corresponding data reported in [11–20].

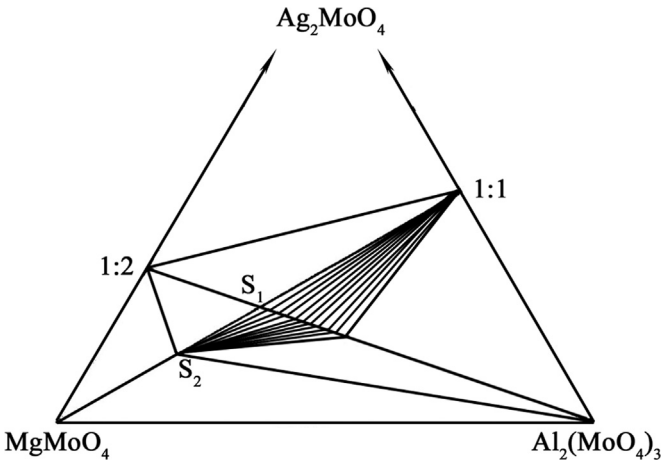

Fig. 1. Subsolidus phase relations at 773 K in the aria $MgMoO_4$–$Ag_2Mg_2(MoO_4)_3$–$AgAl(MoO_4)_2$–$Al_2(MoO_4)_3$ of the system $MgMoO_4$–Ag_2MoO_4–$Al_2(MoO_4)_3$ [8] (S_1 – $Ag_{1-x}Mg_{1-x}Al_{1+x}(MoO_4)_3$, S_2 – $AgMg_3Al(MoO_4)_5$).

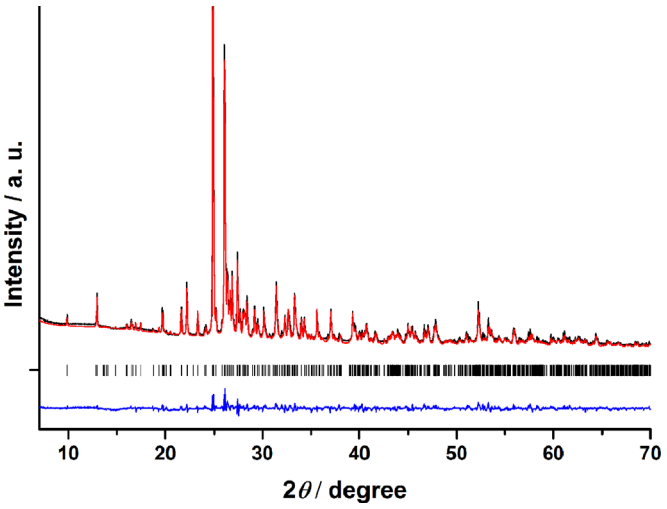

Fig. 2. Diffractogram of sintered sample of $AgMn_3Al(MoO_4)_5$.

Samples of triple molybdates $AgA_3R(MoO_4)_5$ (A=Mg, R=Cr, Fe; A=Mn, R=Al, Cr, Fe, Sc, In) were prepared by annealing stoichiometric mixtures of appropriate simple molybdates at 873–923 K (A=Mg, R=Cr, Fe), 773–853 K (AR=MnAl), 923–973 K

Table 2
Crystal and structure refinement data for $Ag_{0.97}Cr_{1.02}Mg_{2.98}(MoO_4)_5$ and $Ag_{0.95}Fe_{1.04}Mg_{2.96}(MoO_4)_5$.

Formula	$Ag_{0.97}Cr_{1.02}Mg_{2.98}(MoO_4)_5$	$Ag_{0.95}Fe_{1.04}Mg_{2.96}(MoO_4)_5$
Formula weight (g mol^{-1})	1030.50	1032.92
Crystal system	Triclinic	Triclinic
Space group	$P\bar{1}$	$P\bar{1}$
Unit cell dimensions	a=6.8899(3) Å b=6.9598(3) Å c=17.7070(7) Å α=88.002(1)° β=87.301(1)° γ=78.849(1)°	a=6.8987(2) Å b=6.9649(2) Å c=17.7208(4) Å α=88.005(1)° β=87.383(1)° γ=78.859(1)°
V (Å^3); Z	831.85(6) / 2	834.25(4) / 2
Calculated density (g cm^{-3})	4.114	4.112
Crystal size, mm	0.10 × 0.10 × 0.04	0.11 × 0.08 × 0.08
Color	amber	light-yellow
μ(MoK$_\alpha$), mm^{-1}	5.632	5.833
θ range (deg.) for data collection	2.98–37.71	1.15–26.41
Miller index ranges	$-11 \le h \le 11$, $-11 \le k \le 11$, $-27 \le l \le 12$	$-8 \le h \le 8$, $-7 \le k \le 8$, $-21 \le l \le 22$
Reflections collected/ unique	10702/7654 [R(int)=0.0138]	7620/3384 [R(int)=0.0187]
No. of variables	297	297
Goodness-of-fit on F^2 (GOF)	1.052	1.277
Final R indices [$I > 2\sigma(I)$]	$R(F)$=0.0185 $wR(F^2)$=0.0436 $R(F)$=0.0219 $wR(F^2)$=0.0447	$R(F)$=0.0208 $wR(F^2)$=0.0705 $R(F)$=0.0216 $wR(F^2)$=0.0715
R indices (all data)	954	955
Largest difference peak/hole (e Å^{-3})	0.948/−0.907	1.326/−0.968

Table 1
Crystallographic characteristics and melting points of $AgA_3R(MoO_4)_5$.

$A^{II}R^{III}$	Unit cell parameters						V, Å^3	M.p., K
	a, Å	b, Å	c, Å	α, °	β, °	γ, °		
MgAl [8] [a]	6.8570(7)	6.9295(6)	17.619(2)	88.153(9)	87.420(9)	78.891(9)	820.4	1093
MgCr[b]	6.8899(3)	6.9598(3)	17.7070(7)	88.002(1)	87.301(1)	78.849(1)	831.8	1244
MgFe[b]	6.8987(2)	6.9649(2)	17.7208(4)	88.005(1)	87.383(1)	78.859(1)	834.3	1194
MgIn [9] [a]	6.9822(4)	7.0374(5)	17.932(1)	87.642(6)	87.309(6)	79.168(6)	864.0	1303
MnAl	6.9613(4)	7.0240(5)	17.910(1)	87.735(5)	87.439(5)	79.345(6)	859.3	1022
Mn(Al,Mn)[c]	6.9596(6)	7.0326(7)	17.909(6)	87.654(6)	87.442(6)	79.299(7)	860.0	–
MnCr	6.9857(3)	7.0468(4)	17.9801(9)	87.658(4)	87.436(5)	79.243(4)	868.2	1163
MnFe	7.0053(3)	7.0646(4)	18.0132(7)	87.739(4)	87.502(4)	79.295(4)	874.7	1132
MnSc	7.0554(7)	7.1089(7)	18.154(2)	87.406(8)	87.495(9)	79.356(9)	893.4	1297
MnIn	7.0763(6)	7.1265(6)	18.186(1)	87.517(7)	87.551(7)	79.548(8)	900.5	1249
CoAl[d]	6.8547(8)	6.9410(8)	17.597(2)	87.958(6)	87.462(6)	78.818(4)	820.2	–
FeFe [25]	6.928(3)	7.010(6)	17.819(6)	87.66(1)	87.35(1)	79.27(1)	848.9	–

[a] Unit cell parameters are recalculated with the matrix 0 0 −1/1 0 0/0 −1 0.
[b] Single crystal data obtained in this work.
[c] Composition determined in the structure determination is $AgMn^{II}_3(Mn^{III}_{0.26}Al_{0.74})(MoO_4)_5$ [23].
[d] Composition determined in the structure determination is $Ag_{0.90}Al_{1.06}Co_{2.94}(MoO_4)_5$ [24].

Table 3
Atomic coordinates and equivalent isotropic displacement parameters for $Ag_{0.97}Cr_{1.02}Mg_{2.98}(MoO_4)_5$ and $Ag_{0.95}Fe_{1.04}Mg_{2.96}(MoO_4)_5$*.

Atom	Occupancy	*x/a*	*y/b*	*z/c*	U_{eq} (Å^2)**
Mo(1)	1	0.27374(2)	0.30770(2)	0.52720(1)	0.00776(3)
Mo(1)*	1	0.27248(5)	0.30839(4)	0.52696(2)	0.00956(10)
Mo(2)	1	0.21371(2)	0.82595(2)	0.28472(1)	0.00841(3)
Mo(2)*	1	0.21445(4)	0.82658(4)	0.28493(2)	0.01004(11)
Mo(3)	1	0.68801(2)	0.21967(2)	0.30955(1)	0.00978(3)
Mo(3)*	1	0.68605(5)	0.22069(5)	0.30920(2)	0.01154(11)
Mo(4)	1	0.27489(2)	0.05978(2)	0.90528(1)	0.00764(3)
Mo(4)*	1	0.27417(5)	0.06008(4)	0.90519(2)	0.00903(10)
Mo(5)	1	0.24559(2)	0.54770(2)	0.08618(1)	0.00851(3)
Mo(5)*	1	0.24580(5)	0.54744(4)	0.08619(2)	0.00969(10)
M(1)	0.778(3)Mg+0.222(3)Cr	0.18203(7)	0.82799(7)	0.49298(3)	0.00814(1)
M(1)*	0.768(4)Mg+0.232(4)Fe	0.18370(14)	0.82764(14)	0.49279(6)	0.0131(3)
M(2)	0.903(2)Mg+0.097(3)Cr	0.16756(8)	0.08347(8)	0.11603(3)	0.00909(13)
M(2)*	0.828(3)Mg+0.172(3)Fe	0.16875(16)	0.08305(16)	0.11598(6)	0.0157(3)
M(3)	0.793(3)Mg+0.207(3)Cr	0.77857(7)	0.42410(7)	0.12559(3)	0.00798(12)
M(3)*	0.782(4)Mg+0.218(4)Fe	0.77787(15)	0.42401(15)	0.12532(6)	0.0126(3)
M(4)	0.495(3)Mg+0.505(3)Cr	0.24873(5)	0.30622(5)	0.73613(2)	0.00745(9)
M(4)*	0.576(4)Mg+0.424(4)Fe	0.24835(12)	0.30457(12)	0.73545(5)	0.0126(3)
Ag(1)	0.315(9)Ag	0.1452(6)	0.3426(3)	0.2862(5)	0.039(10)
Ag(1)*	0.30(2)Ag	0.1454(16)	0.3442(10)	0.2842(13)	0.041(2)
Ag(2)	0.32(1)Ag	0.1149(4)	0.3365(2)	0.3202(6)	0.0285(11)
Ag(2)*	0.33(3)Ag	0.1132(14)	0.3187(19)	0.32(3)	0.033(4)
Ag(3)	0.334(1)Ag	0.1114(3)	0.3438(4)	0.3425(3)	0.0317(5)
Ag(3)*	0.34(3)Ag	0.1116(9)	0.3420(9)	0.3425(9)	0.0358(14)
O(1)	1	0.5203(2)	0.2105(2)	0.50504(8)	0.0177(3)
O(1)*	1	0.5195(4)	0.2114(4)	0.50497(18)	0.0199(6)
O(2)	1	0.2500(2)	0.3511(2)	0.62456(8)	0.0199(3)
O(2)*	1	0.2488(5)	0.3522(5)	0.62427(17)	0.0225(6)
O(3)	1	0.2020(2)	0.53197(19)	0.47822(8)	0.0153(2)
O(3)*	1	0.2015(4)	0.5325(4)	0.47764(16)	0.0169(6)
O(4)	1	0.12475(19)	0.13213(18)	0.50420(7)	0.0116(2)
O(4)*	1	0.1240(4)	0.1328(4)	0.50399(16)	0.0129(5)
O(5)	1	0.1926(2)	0.8770(2)	0.38029(8)	0.0187(3)
O(5)*	1	0.1935(5)	0.87844(4)	0.38025(16)	0.0202(6)
O(6)	1	0.4586(2)	0.7166(2)	0.26234(8)	0.0174(3)
O(6)*	1	0.4590(4)	0.7165(4)	0.26282(17)	0.0198(6)
O(7)	1	0.1552(2)	0.0511(2)	0.23314(8)	0.0152(2)
O(7)*	1	0.1562(4)	0.0512(4)	0.23277(16)	0.0159(6)
O(8)	1	0.0500(2)	0.6617(2)	0.26703(8)	0.0161(2)
O(8)*	1	0.0509(4)	0.6632(4)	0.26748(17)	0.0188(6)
O(9)	1	0.4429(2)	0.2919(3)	0.33609(9)	0.0253(3)
O(9)*	1	0.4407(5)	0.2939(5)	0.33495(19)	0.0273(7)
O(10)	1	0.8273(2)	0.2040(2)	0.39116(8)	0.0163(2)
O(10)*	1	0.8254(4)	0.2028(4)	0.39099(16)	0.0189(6)
O(11)	1	0.7201(2)	0.9868(2)	0.26923(9)	0.0208(3)
O(11)*	1	0.7175(5)	0.9887(4)	0.26875(18)	0.0229(7)
O(12)	1	0.7680(2)	0.40095(18)	0.24388(7)	0.0120(2)
O(12)*	1	0.7679(4)	0.4007(4)	0.24383(15)	0.0138(5)
O(13)	1	0.2107(2)	0.1132(2)	0.99884(8)	0.0177(3)
O(13)*	1	0.2102(5)	0.1132(4)	0.99877(16)	0.0188(6)
O(14)	1	0.4750(2)	0.0370(2)	0.10619(9)	0.0183(3)
O(14)*	1	0.4754(4)	0.0365(4)	0.10612(17)	0.0195(6)
O(15)	1	0.85544(18)	0.12711(18)	0.11871(7)	0.0106(2)
O(15)*	1	0.8563(4)	0.1267(4)	0.11855(15)	0.0120(5)
O(16)	1	0.23190(18)	0.28788(17)	0.85018(7)	0.0098(2)
O(16)*	1	0.2303(4)	0.2878(4)	0.85023(14)	0.0109(5)
O(17)	1	0.2468(2)	0.5379(2)	0.98816(8)	0.0204(3)
O(17)*	1	0.2471(5)	0.5373(4)	0.98820(16)	0.0218(6)
O(18)	1	0.4787(2)	0.4609(2)	0.12195(9)	0.0192(3)
O(18)*	1	0.4785(4)	0.4611(4)	0.12193(17)	0.0206(6)
O(19)	1	0.1629(2)	0.7935(2)	0.11072(9)	0.0198(3)
O(19)*	1	0.1632(5)	0.7925(4)	0.11046(18)	0.0218(6)
O(20)	1	0.08621(19)	0.38645(18)	0.12350(7)	0.0111(2)
O(20)*	1	0.0873(4)	0.3863(4)	0.12335(5)	0.0130(5)

*The atomic parameters referred to $Ag_{0.95}Fe_{1.04}Mg_{2.96}(MoO_4)_5$ structure are marked with asterisks.
**U_{eq} is defined as one third of the trace of the orthogonalized U_{ij} tensor.

(A=Mn, R=Cr, Fe, In), and 973–1023 K (AR=MnSc), respectively.

Crystals of $AgMg_3R(MoO_4)_5$ (R=Cr, Fe) suitable for structure determinations were obtained by spontaneous crystallization of the melting mixtures of pre-synthesized compounds and $Ag_2Mo_2O_7$ (1:3 molar ratio) cooled from 1123 K to 773 K with the rate of 3–5 K h^{-1} followed by switching off the furnace.

Powder X-ray diffraction (XRD) studies were carried out on automatic diffractometers Bruker D8 Advance (CuK_α radiation, scanning step of 0.02076°) and Thermo ARL (CuK_α, step of 0.02°).

The unit cell dimensions and intensities of diffraction reflections

Table 4
Selected interatomic distances (Å) in $Ag_{0.97}Cr_{1.02}Mg_{2.98}(MoO_4)_5$ and $Ag_{0.95}Fe_{1.04}Mg_{2.96}(MoO_4)_5$.

$Ag_{0.97}Cr_{1.02}Mg_{2.98}(MoO_4)_5$		$Ag_{0.95}Fe_{1.04}Mg_{2.96}(MoO_4)_5$	
Mo(1)-tetrahedron		**Mo(1)-tetrahedron**	
Mo(1)–O(1)	1.735(1)	Mo(1)–O(1)	1.739(3)
–O(2)	1.755(1)	–O(2)	1.757(3)
–O(3)	1.755(1)	–O(3)	1.757(3)
–O(4)	1.809(1)	–O(4)	1.808(3)
< Mo(1)–O >	1.764	< Mo(1)–O >	1.765
Mo(2)-tetrahedron		**Mo(2)-tetrahedron**	
Mo(2)–O(5)	1.735(1)	Mo(2)–O(5)	1.733(3)
–O(6)	1.745(1)	–O(6)	1.746(3)
–O(7)#1	1.773(1)	–O(7)#1	1.776(3)
–O(8)	1.798(1)	–O(8)	1.794(3)
< Mo(2)–O >	1.763	< Mo(2)–O >	1.762
Mo(3)-tetrahedron		**Mo(3)-tetrahedron**	
Mo(3)–O(9)	1.714(2)	Mo(3)–O(9)	1.716(3)
–O(10)	1.761(1)	–O(10)	1.763(3)
–O(11)#2	1.764(2)	–O(11)#2	1.761(3)
–O(12)	1.831(1)	–O(12)	1.829(3)
< Mo(3)–O >	1.768	< Mo(3)–O >	1.767
Mo(4)-tetrahedron		**Mo(4)-tetrahedron**	
Mo(4)–O(13)	1.729(1)	Mo(4)–O(13)	1.731(3)
–O(14)#3	1.730(1)	–O(14)#3	1.734(3)
–O(15)#3	1.790(1)	–O(15)#3	1.790(3)
–O(16)	1.816(1)	–O(16)	1.814(3)
< Mo(4)–O >	1.766	< Mo(4)–O >	1.767
Mo(5)-tetrahedron		**Mo(5)-tetrahedron**	
Mo(5)–O(17)#4	1.739(1)	Mo(5)–O(17)#4	1.740(3)
–O(18)	1.743(2)	–O(18)	1.741(3)
–O(19)	1.758(1)	–O(19)	1.754(3)
–O(20)	1.805(1)	–O(20)	1.802(3)
< Mo(5)–O >	1.761	< Mo(5)–O >	1.759
***M*(1)-octahedron**		***M*(1)-octahedron**	
M(1)–O(5)	2.013(1)	*M*(1)–O(5)	2.014(3)
–O(1)#5	2.018(1)	–O(1)#5	2.015(3)
–O(10)#5	2.055(1)	–O(10)#5	2.062(3)
–O(3)	2.063(1)	–O(3)	2.062(3)
–O(4)#6	2.076(1)	–O(4)#6	2.085(3)
–O(4)#1	2.097(1)	–O(4)#1	2.100(3)
< *M*(1)–O >	2.054	< *M*(1)–O >	2.057
***M*(2)-octahedron**		***M*(2)-octahedron**	
M(2)–O(19)#2	2.030(1)	*M*(2)–O(19)#2	2.037(3)
–O(7)	2.078(1)	–O(7)	2.073(3)
–O(14)	2.080(2)	–O(14)	2.078(3)
–O(20)	2.082(1)	–O(20)	2.085(3)
–O(13)#4	2.091(1)	–O(13)#4	2.092(3)
–O(15)#7	2.111(1)	–O(15)#7	2.117(3)
< *M*(2)–O >	2.079	< *M*(2)–O >	2.080
***M*(3)-octahedron**		***M*(3)-octahedron**	
M(3)–O(17)#5	2.034(2)	*M*(3)–O(17)#5	2.031(3)
–O(18)	2.036(2)	–O(18)	2.035(3)
–O(15)	2.039(1)	–O(15)	2.043(3)
–O(16)#5	2.052(1)	–O(16)#5	2.058(3)
–O(20)#8	2.084(1)	–O(20)#8	2.099(3)
–O(12)	2.084(1)	–O(12)	2.100(3)
< *M*(3)–O >	2.055	< *M*(3)–O >	2.061
***M*(4)-octahedron**		***M*(4)-octahedron**	
M(4)–O(2)	1.989(1)	*M*(4)–O(2)	1.986(3)
–O(6)#5	1.993(2)	–O(6)#5	1.998(3)
–O(11)#5	2.014(2)	–O(11)#5	2.014(3)
–O(16)	2.018(1)	–O(16)	2.033(3)
–O(8)#6	2.030(1)	–O(8)#6	2.036(3)
–O(12)#5	2.030(1)	–O(12)#5	2.079(3)
< *M*(4)–O >	2.012	< *M*(4)–O >	2.024
Ag(1)-environment		**Ag(1)-environment**	
Ag(1)–O(8)	2.210(3)	Ag(1)–O(8)	2.205(8)
–O(9)	2.232(2)	–O(9)	2.225(5)
–O(7)	2.253(2)	–O(7)	2.251(6)
–O(12)#7	2.690(2)	–O(12)#7	2.684(6)
< Ag(1)–O >	2.346	< Ag(1)–O >	2.341

Table 4 (*continued*)

$Ag_{0.97}Cr_{1.02}Mg_{2.98}(MoO_4)_5$		$Ag_{0.95}Fe_{1.04}Mg_{2.96}(MoO_4)_5$	
Ag(2)-environment		**Ag(2)-environment**	
Ag(2)–O(9)	2.251(2)	Ag(2)–O(9)	2.252(6)
–O(8)	2.390(4)	–O(8)	2.388(11)
–O(7)	2.521(7)	–O(7)	2.51(2)
–O(10)#7	2.597(6)	–O(10)#7	2.62(2)
–O(12)#7	2.754(4)	–O(12)#7	2.733(12)
< Ag(2)–O >	2.502	< Ag(2)–O >	2.501
Ag(3)-environment		**Ag(3)-environment**	
Ag(3)–O(9)	2.240(3)	Ag(3)–O(9)	2.229(7)
–O(10)#7	2.458(3)	–O(10)#7	2.471(7)
–O(8)	2.519(3)	–O(8)	2.536(8)
–O(7)	2.824(6)	–O(7)	2.821(14)
< Ag(3)–O >	2.510	< Ag(3)–O >	2.514
Ag(1)–Ag(2)	0.630(7)	Ag(1)–Ag(2)	0.644(17)
Ag(1)–Ag(3)	1.013(7)	Ag(2)–Ag(3)	1.049(19)

Symmetry transformations used to generate equivalent atoms:
#1 x, y+1, z #2 x, y–1, z #3 –x+1, –y, –z+1 #4 x, y, z–1
#5 –x+1, –y+1, –z+1 #6 –x, –y+1, –z+1 #7 x–1, y, z #8 x+1, y, z

for crystal structure determinations of $AgMg_3R(MoO_4)_5$ (R=Cr, Fe) were measured at room temperature on a Bruker-Nonius X8 Apex diffractometer equipped with an area CCD detector (graphite monochromated MoK_α radiation, ϕ scan with a step of $\Delta\phi=0.5^\circ$). Calculations on solution and refinement of the structures were performed with the SHELX-97 program package [21].

Thermoanalytic studies were carried out on a STA 449 F1 Jupiter NETZSCH thermoanalyser (Pt crucible, heating rate of 10 K/min in Ar stream).

The samples were tested by the second-harmonic generation (SHG) method with a laser set-up working in the "reflection" scheme. A minilite-I laser was used as a radiation source of pulsed 1.064 mcm radiation with the repetition rate 15 Hz. In Q-switched mode, the pulse duration was 5 ns with peak light power 0.1 MW. Sensitivity of the installation allowed detecting green light of SHG signal as small as 0.01 of that from the powder α-quartz standard. Such the sensitivity is known [20] to provide 98% reliability in detecting structure acentricity of solids.

Ceramic disks for dielectric investigations were prepared by calcination of pressed powder at 823–853 K for 2 h. The disks were 9–10 mm in diameter and 1–2 mm thick, they were electroded by painting of colloid platinum on their large surfaces with subsequent one hour annealing at about 923 K. The DC electric conductivity was qualitatively controlled with a B7-38 microamperemeter. For quantitative study of the ionic transfer, electric impedance was measured using the two-contact method at frequency 100 Hz in both heating and cooling runs between 298–823 K. The temperature is changed linearly at the rate of 4 K/min. The activation energy of the electric conductivity was calculated from the slope of the straight lines on the Arrhenius plot of the conductivity in the logarithmic scale against the inverse temperature.

3. Results and discussion

3.1. Powder XRD characteristics

The powder XRD patterns of the prepared compounds $AgA_3R(MoO_4)_5$ are similar and show their monophasity and isostructurality to triclinic $NaMg_3In(MoO_4)_5$ (sp. gr. $P\bar{1}$, $Z=2$) [4]. The diffractograms were indexed with taking into account the data obtained later in the course of single crystal structure determination of $AgMg_3R(MoO_4)_5$ (R=Cr, Fe). The result of indexing the XRD pattern for $AgMn_3Al(MoO_4)_5$ is given in Table 1S. The powder XRD pattern of this compound is shown in Fig. 2.

Crystallographic characteristics of the compounds calculated from powder XRD data are listed in Table 1 along with the literature data on other isostructural silver-containing triple molybdates with magnesium and manganese as well as results of structural studies for $AgMn^{II}_3(Mn^{III}_{0.26}Al_{0.74})(MoO_4)_5$ [23] and $Ag_{0.90}Al_{1.06}Co_{2.94}(MoO_4)_5$ [24] crystals belonging to the same structure type.

The obtained and reported data allow us to trace some crystallographic characteristics of $AgA_3R(MoO_4)_5$ in relation to A^{2+} and R^{3+} ions. In magnesium- and manganese-containing triple molybdates, *a, b, c* parameters and the unit cell volumes increase with increasing the trivalent cation radius. With the same trivalent cation, replacement of the smaller Mg^{2+} ion by the larger Mn^{2+} [22] leads to increasing of the unit cell parameters and its volume.

3.2. Crystal structures

The crystal structures of $AgMg_3R(MoO_4)_5$ (R=Cr, Fe) were solved in centrosymmetric sp. gr. $P\bar{1}$, in accordance with no SHG activity of their powders. Thus, all $AgMg_3R(MoO_4)_5$ (R=Cr, Fe) were found to crystallize in the $NaMg_3In(MoO_4)_5$ structure [4]. Final structure data for $AgMg_3R(MoO_4)_5$ (R=Cr, Fe) are listed in Table 2, the positional parameters and equivalent isotropic atomic displacements for both structures are given in Table 3, and selected interatomic distances in Table 4. The populations of four independent positions M=(Mg, R) were refined along with three incompletely occupied Ag sites with keeping the electrical neutrality of the total chemical formula. The final compositions of the crystals are close to stoichiometric $AgMg_3R(MoO_4)_5$ (R=Cr, Fe) with a negligible silver deficiency (Table 2). This deficiency may be connected to close settlement of silver cations in one large cavity with overlapping of electron densities in different silver positions that results in some imaginary lowering of the total silver content. The stoichiometric compositions for triple molybdates of this series were confirmed with the present and previously obtained data on the lack of noticeable homogeneity regions for the compounds at moderate temperatures. However, some deviations from stoichiometry with small silver deficiency cannot be excluded at higher temperatures.

The most pronounced deviation was observed for $Ag_{0.90}Al_{1.06}Co_{2.94}(MoO_4)_5$ [24], which can be caused by essentially higher crystallization temperature of this phase compared with our

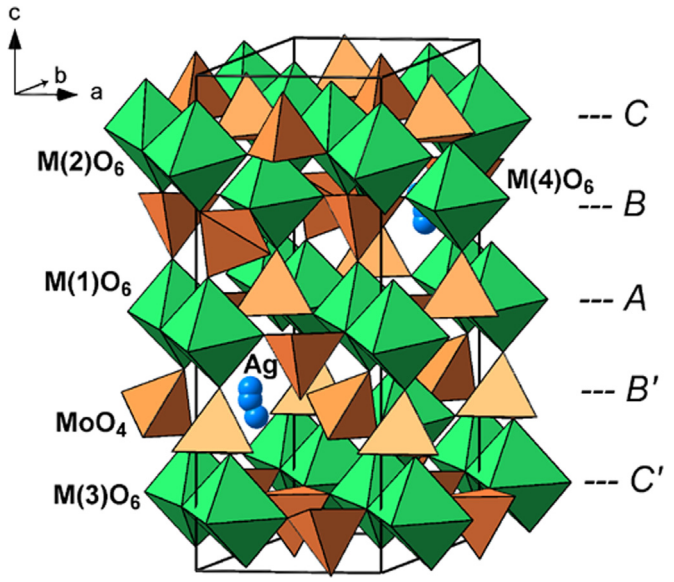

Fig. 3. A general view of $AgMg_3Cr(MoO_4)_5$ structure.

conditions. The formation of $AgMn^{II}_3(Mn^{III}_{0.26}Al_{0.74})(MoO_4)_5$ [23] can also be explained by relatively extreme crystallization conditions with oxidation of Mn(II) to Mn(III) in the melt. However, the Mn^{III} content in this crystal appears to be substantially overestimated by the authors.

In the structures of $AgMg_3R(MoO_4)_5$ (R=Cr, Fe), all the atoms are located in general positions. Five crystallographically independent Mo atoms have a tetrahedral coordination with the Mo–O distances of 1.714(2)–1.831(1) and 1.716(3)–1.829(1) Å in $AgMg_3Cr(MoO_4)_5$ and $AgMg_3Fe(MoO_4)_5$, respectively. Three Mg^{2+} cations and one R^{3+} cation are statistically distributed on octahedral $M(1)$–$M(4)$ positions noticeably differing in Mg/R ratios with the (Mg, Cr)–O and (Mg, Fe)–O bond lengths of 1.989(3)–2.111(1) and 1.986(3)–2.118(1) Å, respectively. The average M–O values agree well with the corresponding populations (Tables 3 and 4) and are intermediate between those for the bond lengths Mg–O, Cr–O and Fe–O in the structures of $MgMoO_4$ [12], α-$Cr_2(MoO_4)_3$ [26], and α-$Fe_2(MoO_4)_3$ [27].

It is interesting to consider coordinations and disordering of Ag^+ ions. In the first approximation, the silver atoms in $AgMg_3R(MoO_4)_5$ (R=Cr, Fe) have 3 or 4 nearest oxygen atoms (Table 4). The Ag atoms are inside the sphere of radius 2.7 Å which is approximately equal to the mean Ag–O bond length for CN=8 [22] and corresponds the bond valence sum [28] $s \approx 0.1$. However, there are some Ag–O distances in the range 2.7–2.9 Å, making us to accept CN=3+1 for Ag(1), Ag(3) and 4+1 for Ag(2). Average Ag–O bond lengths for the last coordinations increase in the row Ag(1)–Ag(2)–Ag(3) while corresponding occupancies stay close. Analogous coordinations and disordering of Ag^+ and Na^+ ions were also found in $AgMn^{II}_3(Mn^{III}_{0.26}Al_{0.74})(MoO_4)_5$ [23], $Ag_{0.90}Al_{1.06}Co_{2.94}(MoO_4)_5$ [24] and $NaMg_3In(MoO_4)_5$ [4]. Splitting of the Ag positions in similar irregular oxygen environments of Ag^+ are also found in $Ag_2A_2(MoO_4)_3$ (A=Mg, Mn, Co, Zn) [29–31]. According to [31], such disorder of Ag^+ in the latter compounds indicates higher silver-ion mobility at elevated temperatures.

In the structures of $AgMg_3R(MoO_4)_5$ (R=Cr, Fe), MoO_4 tetrahedra, couples of edge-shared $M(1)O_6$ octahedra, and trimers of edge-shared $M(2)O_6$, $M(3)O_6$ and $M(4)O_6$ octahedra are linked by the common vertices to form a 3D framework (Fig. 3). According to [5,23,24], the framework organization is conveniently described as a stacking of polyhedral layers along c axis. One can separate three sorts of the adjacent layers, A, B and C (Fig. 4), as well as B' and C'

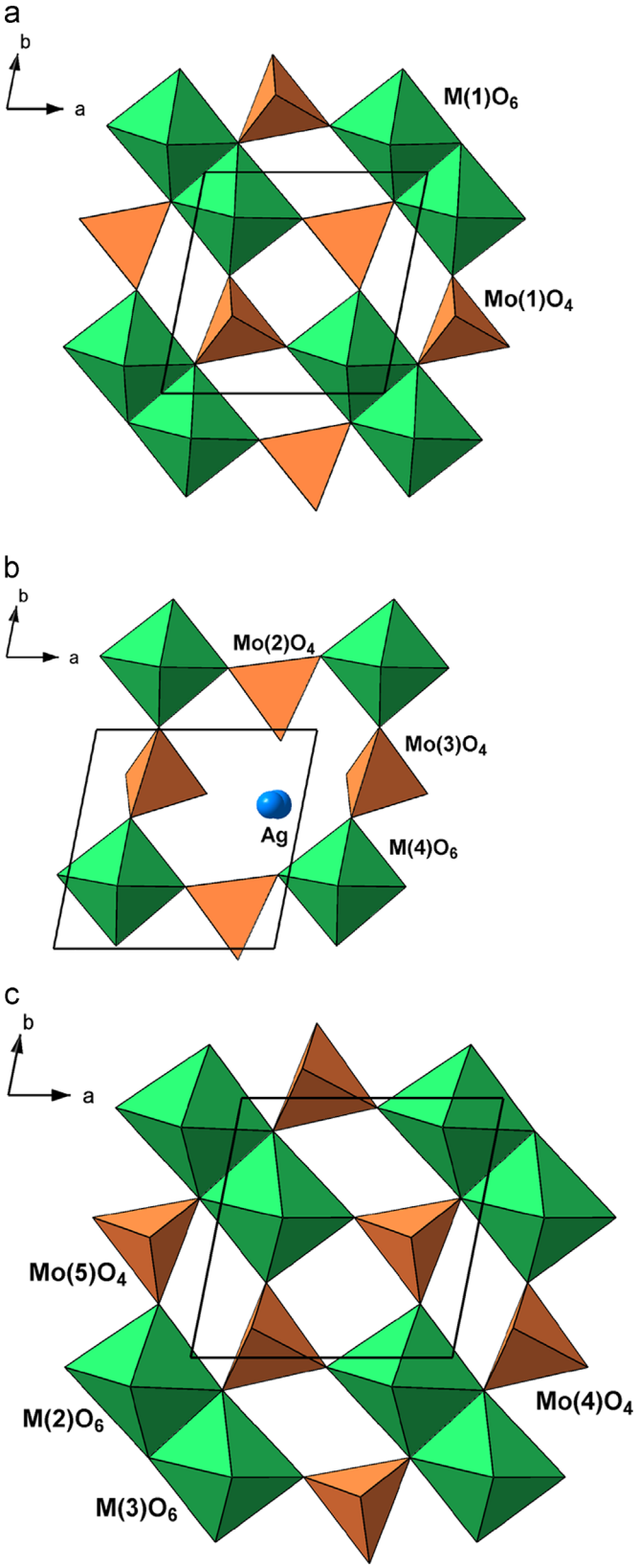

Fig. 4. Three kinds of polyhedral layers in the structures of $AgMg_3R(MoO_4)_5$ (R=Cr, Fe): *a* – layer *A*; *b* – layer *B*; *c* – layer *C*.

layers inverted relative to *B* and *C* layers. These polyhedral layers are stacked in sequence *A*–*B*–*C*–*C′*–*B′*–*A*… (Fig. 3) via the bridge MoO_4 tetrahedra (the layers *A* and *B*, *A* and *B′*, *C* and *C′*) or via the vertices of the bridge $Mo(2)O_4$ and $Mo(3)O_4$ tetrahedra and the

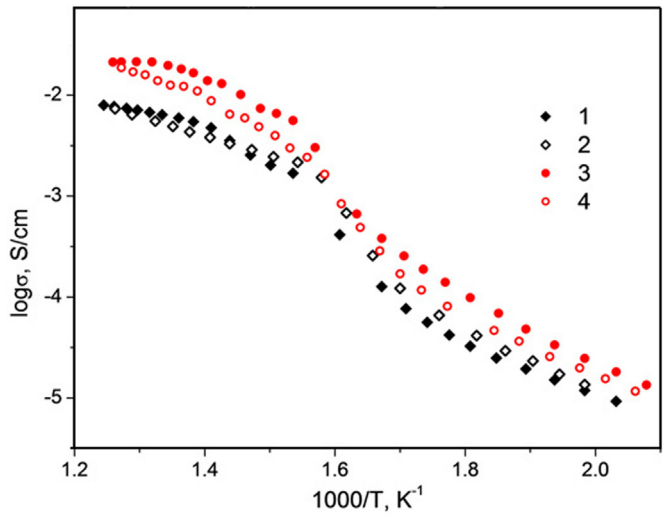

Fig. 5. Temperature dependences of electric conductivity on heating (closed symbols) and cooling (open symbols) at 100 Hz for $AgMn_3Al(MoO_4)_5$ (1, 2) and $AgMg_3Al(MoO_4)_5$ (3, 4).

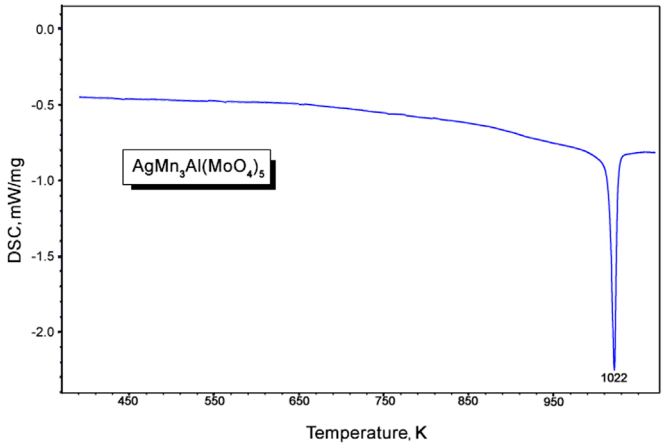

Fig. 6. DSC curve for polycrystalline $AgMn_3Al(MoO_4)_5$ on heating.

common edges of the $M(3)O_6$ and $M(4)O_6$ octahedra (the layers B and C, B' and C'). The A and B layers are also encountered in the structures of α-$MFe_2(MoO_4)_3$ (M=Na, Ag) [5,32] in the sequence A–B–B'–A…, whereas in β-$NaFe_2(MoO_4)_3$ [5] we have B–[B']–[B]–B'–B…, where [B] is the layer B with no cation at the centre of the polyhedral ring. As seen in Fig. 4c, the polar C layer differs from the similar centrosymmetrical A layer in that all MoO_4 tetrahedra point upwards. This manner allows the C and C' layers to be connected to each other by an inversion operation.

In the large framework cavities, the silver cations are disordered on three close positions with the distances Ag–Ag 0.630(7) and 1.014(7) Å in $AgMg_3Cr(MoO_4)_5$, and 0.65(1) and 1.04(1) Å in $AgMg_3Fe(MoO_4)_5$. Such a disordering is also typical for other compounds of this isostructural series [4–6,23,24], suggesting a possible mobility of the Na^+ or Ag^+ cations in the compounds. This is favored not only by defects in Na and Ag positions along with their irregular coordination but also a rather flexible polyhedral framework of the $NaMg_3In(MoO_4)_5$ structure type which involves communicative cavities. An analysis of the out-of-framework space in $AgMg_3R(MoO_4)_5$ (R=Cr, Fe) structures indicates that the most vast cavity is settled by Ag(3) atom. There are also quadrangular windows of alternating MO_6 octahedra and MoO_4 tetrahedra with minimal distances O…O 3.7–4.0 Å, which could be penetrable for Ag^+ ions at elevated temperatures. This provides good conditions for fast Ag^+ mobility within the B and B' layers, and suggests 2D character of silver-ion conductivity. Obviously, the same character of ionic conductivity may be expected for sodium-containing compounds in the $NaMg_3In(MoO_4)_5$ family.

3.3. Electric conductivity

Platinum electrodes on ceramic samples $AgA_3Al(MoO_4)_5$ (A=Mn, Mg) are blocking for direct current (DC) electric conductivity as it was demonstrated with the V-38 device. This means that electronic conductivity in temperature region of 473–773 K is negligible in comparison with alternating current (AC) conductivity (σ) measured at frequency 100 Hz (Fig. 5). It is seen that near RT conductivity is small as 10^{-6} S/cm but quickly rises with temperature to values of about 10^{-2} S/cm. Similar behavior is also typical for many good sodium-ion conductors by of the NASICON family. It is meaningful that conductivity of $AgA_3Al(MoO_4)_5$ (A=Mn, Mg) increases with temperature in non-monotonic way showing distinct breaks on lg $\sigma = f(1/T)$ curves at 653 K for $AgMg_3Al(MoO_4)_5$ and at 683 K for $AgMn_3Al(MoO_4)_5$ though there are no strongly pronounced thermal effects near these temperatures, at least for $AgMn_3Al(MoO_4)_5$ (Fig. 6). At higher temperatures the dependences lg $\sigma = f(1/T)$ are almost linear with small activation energies E_a=0.39 eV for the first, and E_a=0.65 eV for the second of these substances, respectively, on cooling. In the case of heating the dependences are not so indicative probably because of near electrode area relaxation processes. Above 653 K, the electric conductivity of $AgMg_3Al(MoO_4)_5$ increases up to $2.5 \cdot 10^{-2}$ S/cm at 773 K, being a rather high value even in comparison with those in the NASICON family.

Quick rise of σ with reaching high electric conductivity in both compounds under study goes through temperature regions where we may expect phase transitions which nevertheless are not marked with sharp thermo-effects on DTA curves because of rather broad intervals of their passing (588–653 K for A=Mg and 603–683 K for A=Mn). Such strongly diffused first- or second-order phase transition are not unusual in ionic conductors with mixed crystal frameworks especially those involving aliovalent substituting ions, e.g. $Na_{1+x}Zr_2P_{3-x}Si_xO_{12}$ ($0 < x < 3$) [33], $Li_{1-x}Zr_{2-x}Ta_x(PO_4)_3$ [34].

A comparison of electric conductivities of triple molybdates $AgA_3Al(MoO_4)_5$ (A=Mn, Mg) reveals an influence of the cation substitutions on electro-conductive properties. It follows from the data that $AgMg_3Al(MoO_4)_5$ with smaller cation Mg^{2+} exhibits higher electrical conductivity at elevated temperatures compared to $AgMn_3Al(MoO_4)_5$. Probably, lesser difference between radii of Mg^{2+} and Al^{3+} cations (0.86 and 0.67 Å, respectively, against 0.97 Å for Mn^{2+} [22]) better provides adjustment by sizes of AO_6 and AlO_6 octahedra and smoothing of potential relief along the fast-ion conduction paths in $AgA_3Al(MoO_4)_5$ where AO_6 and AlO_6 octahedra interchange. Another explanation is a redistribution of A^{2+} and R^{3+} cations over the M positions in $AgA_3R(MoO_4)_5$ at elevated temperatures that can create the additional steric barriers for the Ag^+ ions. Clearly, these barriers are lower for Mg^{2+} and Al^{3+} in $AgMg_3Al(MoO_4)_5$ than for Mn^{2+} and Al^{3+} in $AgMn_3Al(MoO_4)_5$.

Acknowledgments

The authors are grateful to Dr. I.A. Gudkova for obtaining single crystal XRD data for $AgMg_3R(MoO_4)_5$ (R=Cr, Fe), and Mrs. Tamara S. Yudanova for English translation of the paper.

This study was supported by the Russian Foundation for Basic Research, Grants Nos. 13-03-01020 and 14-03-00298.

Appendix A. Supplementary material

Supplementary data associated with this article can be found in the online version at http://dx.doi.org/10.1016/j.jssc.2016.03.003.

References

[1] B.I. Lazoryak, V.A. Efremov, The variable-composition $Na_{2x}M_2^{II}Sc_{2(1-x)}(MoO_4)_3$ phases (M=Zn, Cd, Mg), Zhurnal Neorg. Khimii 32 (1987) 652–656, in Russian.

[2] N.M. Kozhevnikova, I.Yu. Kotova, Triple molybdates $NaA_3R(MoO_4)_5$ (A=Mg, Mn, Co, Ni; *R*=Al, In, Cr, Fe) – representatives of a new structural family, Zhurnal Neorg. Khimii 42 (1997) 17–19, in Russian.

[3] N.M. Kozhevnikova, I.Yu. Kotova, X-ray study of phases of variable-composition $M_{1-x}A_{1-x}R_{1+x}(MoO_4)_3$, $0 \le x \le 0.3$–0.5 (M=Na, K; A=Mg, Mn, Co, Ni; *R*=Al, In, Cr, Fe, Sc), Zhurnal Neorg. Khimii 45 (2000) 102–103, in Russian.

[4] R.F. Klevtsova, A.D. Vasiliev, N.M. Kozhevnikova, L.A. Glinskaya, A.I. Kruglik, I. Yu. Kotova, Synthesis and crystal structural study of ternary molybdate $NaMg_3In(MoO_4)_5$, J. Struct. Chem. 34 (1994) 784–788.

[5] E. Muessig, K.G. Bramnik, H. Ehrenberg, Structural investigation in the Na–Fe–Mo–O system, Acta Cryst. B59 (2003) 611–616.

[6] K. Hermanowicz, M. Maczka, M. Wolcyrz, P.E. Tomaszewski, M. Paściak, J. Hanuza, Crystal structure, vibrational properties and luminescence of $NaMg_3Al(MoO_4)_5$ crystal doped with Cr^{3+} ions, J. Solid State Chem. 179 (2006) 685–695.

[7] I.Yu. Kotova, Phase formation in the Ag_2MoO_4–$CoMoO_4$–$Al_2(MoO_4)_3$ system, Russ. J. Inorg. Chem. 59 (2014) 844–848.

[8] I.Yu. Kotova, V.P. Korsun, Phase formation in the Ag_2MoO_4–$MgMoO_4$–$Al_2(MoO_4)_3$ system, Russ. J. Inorg. Chem. 55 (2010) 955–958.

[9] I.Yu. Kotova, V.P. Korsun, Phase formation in the system involving silver, magnesium, and indium molybdates, Russ. J. Inorg. Chem. 55 (2010) 1965–1969.

[10] I.Yu. Kotova, D.A. Belov, S.Yu. Stefanovich, $Ag_{1-x}Mg_{1-x}R_{1+x}(MoO_4)_3$ Ag^+-conducting NASICON-like phases, where R=Al or Sc and $0 \le x \le 0.5$, Russ. J. Inorg. Chem. 56 (2011) 1189–1193.

[11] R. Kohlmuller, J.-P. Faurie, Etude des systemes MoO_3–Ag_2MoO_4 et MoO_3–MO (M – Cu, Zn, Cd), Bull. Soc. Chim. 11 (1968) 4379–4382.

[12] V.V. Bakakin, R.F. Klevtsova, L.A. Gaponenko, Crystal structure of magnesium molybdate $MgMoO_4$, an example of a modified close packing with two types of tetrahedra, Kristallografiya 27 (1982) 38–42, in Russian.

[13] V.K. Trunov, L.M. Kovba, On interaction of trioxides of molybdenum and tungsten with sesquioxides of iron and chromium, Izv. Akad. Nauk SSSR Neorg. Mater. 2 (1966) 151–154, in Russian.

[14] E.I. Get'man, V.I. Marchenko, Phase equilibria in the systems $Bi_2(MoO_4)_3$–$Me_x(MoO_4)_y$ (Me=Ni, Co, Mn, Al, Cr, Fe, In), Zhurnal Neorg. Khimii 28 (1983) 713–718, in Russian.

[15] P. Rajaram, B. Viswanathan, G. Aravamudan, V. Srinivasan, M.V.C. Sastri, Studies on the formation of manganese molybdates, Thermochim. Acta 7 (1973) 123–129.

[16] W.P. Doyle, G. McGuire, G.M. Clark, Preparation and properties of transition metal molybdates (VI), J. Inorg. Nucl. Chem. 28 (1966) 1185–1190.

[17] L.M. Plyasova, L.M. Kefeli, X-ray study of chromium and aluminum molybdates, Izv. Akad. Nauk SSSR Neorg. Mater. 3 (1967) 906–908, in Russian.

[18] V.K. Trunov, L.M. Kovba, The reaction of In_2O_3 with WO_3 and MoO_3, Vestnik Moskovskogo universiteta. Khimiya 1 (1967) 114–115, in Russian.

[19] V.K. Trunov, N.P. Anoshina, L.N. Komissarova, X-ray study of molybdate and tungstate of scandium, Zhurnal Neorg. Khimii 12 (1967) 2856–2857, in Russian.

[20] S.K. Kurtz, J.P. Dougherty, Method for the detection of noncentrosymmetry in solids, Systematic Material Analysis, Springer Verlag, N.Y., 1978. vol. 4, Ch. 38. pp. 269–342.

[21] G.M. Sheldrick, SHELX97, Release 97-2. Göttingen, Germany: Univ. of Göttingen, 1997.

[22] R.D. Shannon, Revised effective ionic radii and systematic studies of interatomic distances in halides and chalcogenides, Acta Cryst. 32 (1976) 751–767.

[23] C. Bouzidi, W. Frigui, M.F. Zid, Synthèse et structure cristalline d'un matériau noir $AgMn_3^{II}(Mn_{0.26}^{III}Al_{0.74})(MoO_4)_5$, Acta Cryst. E71 (2015) 299–304.

[24] R. Nasri, S.F. Chérif, M.F. Zid, Structure cristalline de la triple molybdate $Ag_{0.90}Al_{1.06}Co_{2.94}(MoO_4)_5$, Acta Cryst. E71 (2015) 388–391.

[25] L.V. Balsanova, Synthesis of crystals of silver containing oxide phases based on molybdenum, study of their structure and properties, Vestnik VSGUTU 5 (2015) 63–69, in Russian.

[26] P.D. Battle, A.K. Cheetham, W.T.A. Harrison, N.J. Pollard, J. Faber Jr., The structure and magnetic properties of chromium(III) molybdate, J. Solid State Chem. 58 (1985) 221–225.

[27] P.D. Battle, A.K. Cheetham, G.J. Long, G. Longworth, Study of the magnetic properties of iron(iii) molybdate, by susceptibility, Moessbauer, and neutron diffraction techniques, Inorg. Chem. 21 (1982) 4223–4228.

[28] I.D. Brown, D. Altermatt, Bond-valence parameters obtained from a systematic analysis of the inorganic crystal structure database, Acta Cryst. B41 (1985) 244–247.

[29] C. Gicquel-Mayer, M. Mayer, G. Perez, Etude structurale du molybdate double d'argent et de zinc $Ag_2Zn_2Mo_3O_{12}$, Acta Cryst. B37 (1981) 1035–1039.

[30] G.D. Tsyrenova, S.F. Solodovnikov, E.G. Khaikina, E.T. Khobrakova, Phase formation in the Ag_2O–MgO–MoO_3 system and the crystal structure of new double molybdate $Ag_2Mg_2(MoO_4)_3$, Russ. J. Inorg. Chem. 46 (2001) 1886–1891.

[31] G.D. Tsyrenova, S.F. Solodovnikov, E.G. Khaikina, E.T. Khobrakova, Zh. G. Bazarova, Z.A. Solodovnikova, Phase formation in the systems Ag_2MoO_4–MO–MoO_3 (M=Ca, Sr, Ba, Pb, Cd, Ni, Co, Mn) and crystal structures of $Ag_2M2(MoO_4)_3$ (M=Co, Mn), J. Solid State Chem. 177 (2004) 2158–2167.

[32] L. Balsanova, D. Mikhailova, A. Senyshyn, D. Trots, H. Fuess, W. Lottermoser, H. Ehrenberg, Structure and properties of α–$AgFe_2(MoO_4)_3$, Solid State Sci. 11 (2009) 1137–1143.

[33] S. Yde-Andersen, J.S. Lundsgaard, L. Moller, J. Engell, Properties of NASICON electrolytes prepared from alkoxide derived gels: ionic conductivity, durability in molten sodium and strength test data, Solid State Ion. 14 (1984) 73–79.

[34] I.A. Stenina, M.G. Zhizhin, B.I. Lazoryak, A.B. Yaroslavtsev, Phase transitions, structure and ion conductivity of zirconium hydrogen phosphates, $H_{1\pm x}Zr_{2-x}M_x(PO_4)_3 \cdot H_2O$ (M=Nb, Y), Mater. Res. Bull. 44 (2009) 1608–1612.